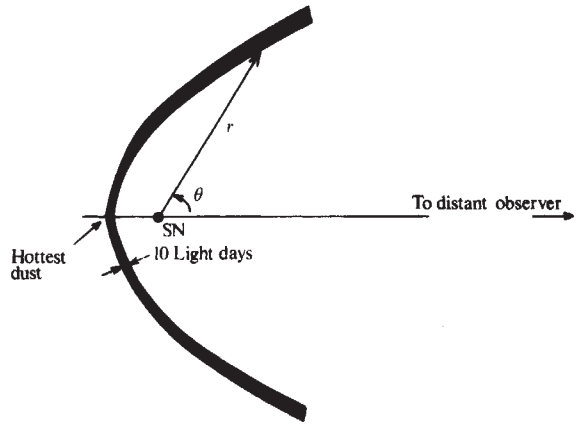

Fig. 3 The paraboloidal shell $r = ct/(1-\cos\theta)$ of hot dust from which a distant observer receives IR radiation.

the grains,

$$\frac{L_{SN}}{4\pi r^2}\bar{Q}(a, T_{SN})\pi a^2 = 4\pi a^2 \bar{Q}(a, T_g)\sigma T_g^4 \quad (1)$$

where r is the SN-hot grain distance, $\bar{Q}(a, T)$ the Planck average emissivity, a the grain radius, T_{SN} the colour temperature of the SN photosphere, T_g the grain temperature, derived from the IR colours assuming a λ^{-1} emissivity law, and σ Stefan's constant. We have assumed that the optical properties of the grains are described by $\bar{Q}/a \propto T_g$. For illustration we have used the values for $\bar{Q}$ quoted by Draine[16] for carbon. (Use of a dielectric grain material such as silicate[16] does not affect our conclusions.) Rearranging equation (1) and substituting typical numerical values, we obtain

$$r = 7.2\times10^{24}\, T_g^{-5/2}\left(\frac{a}{0.1\ \mu m}\right)^{-1/2}\left(\frac{L_{SN}}{10^{43}\ erg\ s^{-1}}\right)^{1/2} cm \quad (2)$$

The observed change in grain temperature is interpreted as being due to the increasing distance, r, at which the heated grains lie. The distances inferred by this method are presented in Fig. 2, plotted against time. A straight line fits these points well, and gives as the gradient a constant velocity

$$v = (2.2\pm0.2)\times10^5\left(\frac{a}{0.1\ \mu m}\right)^{-1/2}\left(\frac{L_{SN}}{10^{43}\ erg\ s^{-1}}\right)^{-1/2} km\ s^{-1} \quad (3)$$

For typical values of a (ref. 17) and L_{SN} (ref.14) this velocity is comparable to the speed of light. The echo model predicts this result. In general when a source 'switches on' in a dust cloud, light travel-time arguments show[9] that the grains from which a distant observer receives IR emission lie within a paraboloid of revolution $r = ct(1-\cos\theta)^{-1}$ (Fig. 3). For a pulse-like light curve this heated dust is confined within the shell as shown in Fig. 3. For a given paraboloid the temperature distribution is such that the hottest dust is situated at the vertex ($r = ct/2$, $\theta = \pi$), the point closest to the SN. Integrating the flux from the paraboloidal shell, one can show that nearly all the flux comes from this hot region around the vertex providing that the observations are made on the Wien slope of the thermal emission; for example, if the dust at the vertex has a temperature of 1,000 K and observations are made at 2.2 μm, 90% of the flux comes from within 30° of the vertex. Cooler grains further from the SN do not contribute significantly to our measurements. The expected recession velocity of the vertex

$$\frac{\partial}{\partial t}\left(\frac{ct}{1-\cos\theta}\right)\Big|_{\pi} = \frac{c}{2}$$

consistent with the determined velocity v. In addition, extrapolation of the graph back to $t = 0$ gives $r = 0$ within the errors. The linearity, gradient and (0, 0) intercept of the r versus t graph are all strong evidence for the echo model. Detailed numerical modelling (J.R.G. *et al.*, in preparation) of a SN embedded in a Betelgeuse-type dust cloud of $\tau_{UV-VIS} \sim 0.1$, mass $\sim 10^{-2} M_\odot$ and radius $\sim 10^{18}$ cm shows that the observed IR light curves are reproduced.

We conclude that the IR emission from SN 1982g was due to a pre-existing circumstellar dust shell heated by the SN pulse. This is the first clear evidence for the occurrence of an IR echo in any source.

We thank Dr Bob Joseph and Dr Norna Robertson for valuable comments and suggestions, and Mr David King for efficient measuring of star positions. We are also grateful for the support provided by the staffs of the AAO, RGO and UKIRT. J.R.G. thanks the Department of Education for Northern Ireland for a research studentship and travel funds. G.P. thanks the University of Keele for a research studentship and the SERC for travel funds. M.F.B. is supported by the US Department of Energy.

Note added in proof; Dwek[18] has recently interpreted the IR light curves of both SN 1979c and SN 1980k as being due to an echo of the UV–visual output of the SN.

Received 25 May; accepted 6 July 1983.

1. Maza, J. *IAU Circ.* No. 3684 (1982).
2. de Vaucouleurs, G. & de Vaucouleurs, A. *Second Reference Catalogue of Bright Galaxies* (University of Texas Press, 1976).
3. Cowal, C. T. *The Palomar Supernova Search Master List* (Caltech, 1982).
4. Merrill, K. *IAU Circ.* No. 3444 (1980).
5. Dwek, E. *et al. Bull. Am. astr. Soc.* **13,** 795 (1981).
6. Chevalier, R. A. *Astrophys. J.* **251,** 259–265 (1981).
7. Cernuschi, E., Marsicano, F. & Codina, S. *Ann. Astrophys.* **30,** 1039–1051 (1967).
8. Hoyle, F. & Wickramasinghe, N. C. *Nature* **226,** 62–63 (1970).
9. Bode, M. F. & Evans, A. *Astr. Astrophys.* **73,** 113–120 (1979).
10. Weiler, K. W., Sramek, R. A., van der Hulst, J. M. & Panagia, N. in *Supernovae: A Survey of Current Research,* 281–291 (Reidel, Dordrecht, 1982).
11. Branch, D. *et al. Astrophys. J.* **244,** 780–804 (1981).
12. McMillan, R. S. & Tapia, S. *Astrophys. J. Lett.* **226,** L87–L89 (1978).
13. Morrison, P. & Sartori, L. Astrophys. J. **158,** 541–570 (1969).
14. Colgate, S. A., Petschek, A. K. & Kriese, J. T. *Astrophys. J. Lett.* **237,** L81–L85 (1980).
15. Panagia, N. *et al. Mon. Not. R. astr. Soc.* **192,** 861–879 (1980).
16. Draine, B. T. *Astrophys. J.* **245,** 880–890 (1981).
17. Rowan-Robinson, M. & Harris, S. *Mon. Not. R. astr. Soc.* **200,** 197–215 (1982).
18. Dwek, E. *Astrophys. J.* (in the press).

A two-stage mechanism for escape of Na and K from Io

Michael E. Summers*, Yuk L. Yung* & Peter K. Haff†

* Division of Geological and Planetary Science, and † Division of Physics, Mathematics and Astronomy, California Institute of Technology, Pasadena, California 91125, USA

It is generally accepted that Io is the source of S, O, Na and K which, after ionization, form the constituents of the Io plasma torus. The escape of S and O from Io can be understood in terms of the photochemistry of a predominantly SO_2 atmosphere created by the high vapour pressure of SO_2 (refs 1, 15). However, the vapour pressures of Na_2S, K_2S and other common compounds containing Na and K are negligible at the surface temperatures of Io. This has given rise to the suggestion that over part of Io's surface (the nightside) the atmosphere is thin enough so that surface sputtering by co-rotating ions can eject Na and K directly into the Io torus[2,3]. The main objection to this idea is that it implies a 'Sun-locked' source for Na and K, while observations of the Na and K clouds around Io indicate a 'Jupiter-locked' ejection mechanism. We propose here that Na and K escape from Io in two stages. Atoms of Na and K are first sputtered into the atmosphere from the surface by high-energy magnetospheric ions. Atmospheric sputtering[4] by low-energy co-rotating ions then removes these constituents (along with others present) out of Io's gravitational field. We suggest that the observed Na and K ejection asymmetry is due to preferential sputtering of atmospheric particles on the hemisphere of Io facing Jupiter. The estimated injection rates are sufficiently large to maintain the observed K, Na, and O clouds observed around Io[5–7,18].

0028–0836/83/340710—03$01.00

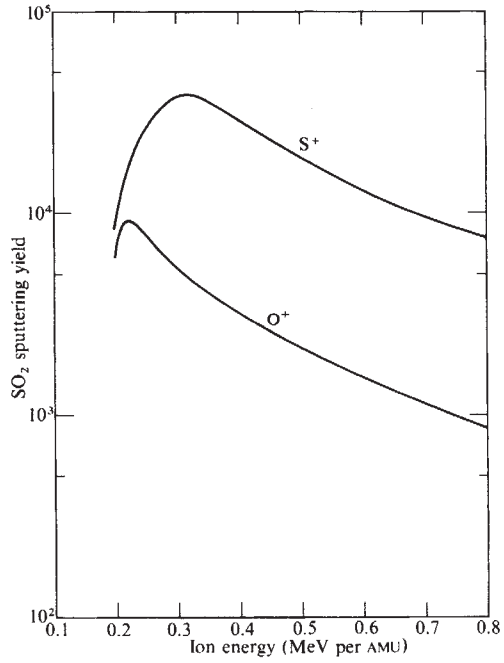

Fig. 1 The calculated SO_2 sputtering yield as a function of incident energy for S^+ and O^+ ions. The calculations were performed using the theory of Watson and Tombrello[12].

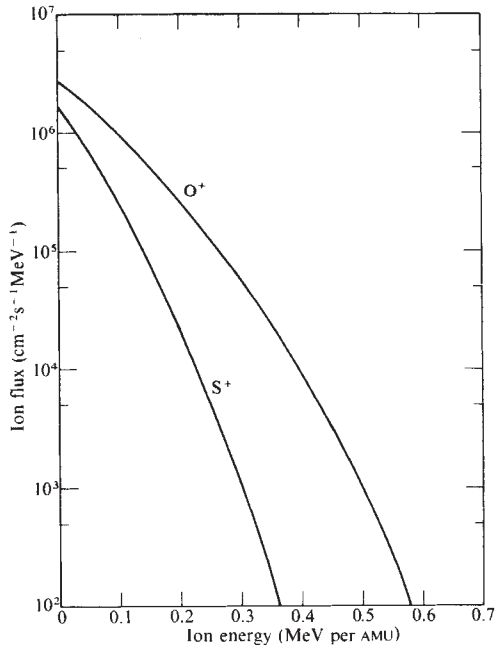

Fig. 2 The differential ion flux in the vicinity of Io's orbit, adopted from Lanzerotti *et al.*[10], and extrapolated to higher energies using the power law $d(flux)/dE = (E/E_0)^{-n}$, where E_0 is a reference energy and $n = 7$.

The SO_2 abundance of 0.2 cm atm detected by the Voyager I IRIS experiment in the subsolar region of Io corresponds to a SO_2 vertical column density $N_{IRIS} \simeq 5 \times 10^{18}$ cm^{-2} (ref. 8). This is approximately the atmospheric SO_2 abundance that would exist if the SO_2 gas were in thermodynamic equilibrium with SO_2 surface frost at $T = 130$ K. The globally-averaged SO_2 vertical column density $\bar{N}$ is probably much less than this value since the vapour pressure of SO_2 decreases exponentially with decreasing temperature. An estimate of $\bar{N}$ may be obtained by assuming local pressure equilibrium between atmospheric SO_2 and surface frost. From an extrapolation of the SO_2 vapour pressure data of D. D. Wagman (personal communication), and a surface temperature variation which approximates the IRIS observations[8], we obtain $\bar{N} \simeq 5 \times 10^{17}$ cm^{-2}. Note that photochemical models of Io's atmosphere which reproduce the characteristics of the downstream ionosphere as observed by Pioneer 10 require $\bar{N} \geq 1 \times 10^{17}$ cm^{-2} (ref. 9).

Co-rotating S^+ and O^+ ions in the plasma torus impacting Io's atmosphere are unable to penetrate to Io's surface if $\bar{N} \geq 10^{16}$ cm^{-2} (ref. 10). In order for S^+ and O^+ ions to penetrate an SO_2 atmosphere characterized by $\bar{N} \simeq 5 \times 10^{17}$ cm^{-2}, their incident kinetic energies must be greater than 0.3 MeV and 0.1 MeV, respectively. The Voyager I low-energy charged particle (LECP) and plasma science (PLS) experiments detected a flux $F \simeq 10^5$ cm^{-2} s^{-1} MeV^{-1} of ions in the vicinity of Io's orbit with energies greater than these minimum values[10].

The sputtering of frozen SO_2 frost by high-energy ($0.08 \leq E$ (MeV per AMU) ≤ 1.30) He and F ions has recently been studied by Melcher *et al.*[11] (see also ref. 10). The peak sputtering yield for incident F^+ was 7,300 at energy $E_p = 0.32$ MeV per AMU. The yield spectrum exhibited a rapid rise with increasing energy for $E < E_p$, and an exponential decrease for $E > E_p$. The qualitative character of the yield spectrum was previously predicted on the basis of a modified lattice potential model of high-energy ion erosion developed by Watson and Tombrello[12]. The theory correctly predicts the energy at which the peak yield occurs; however, the magnitude of the predicted yields is a factor of ~3 too large. We have utilized this theory to estimate the sputtering yield due to impacting high energy O^+ and S^+ on SO_2. In Fig. 1 we show the calculated yields as a function of incident ion energy, E, made using the same normalization factor that adjusted the calculated F^+ sputtering yields to agree with the data. The peak yield for O^+ on SO_2 frost is 8,900 and occurs at $E = 0.23$ MeV per AMU. The sputtering yield spectra for F^+ and O^+ are similar because they have similar masses. The peak yield for S^+ on SO_2 frost is 35,000 at $E = 0.4$ MeV per AMU.

The surface sputtering rate due to impacting ions is given by the integral of the product of the yield and the differential ion flux incident on the surface. The differential ion flux in the vicinity of Io's orbit was measured by the Voyager I PLS and LECP experiments; however, the composition of the high-energy plasma is uncertain. We have used the PLS and LECP data and data extrapolations of the high-energy ion flux given by Lanzerotti *et al.* (ref. 10, and see Fig. 2), to calculate the surface sputtering rate on Io. Assuming that the high-energy ions consist of S^+ and O^+ in the ratio 1:2, we find a surface sputtering rate $\phi_{SO_2} \simeq 8 \times 10^8$ cm^{-2} s^{-1}. This value of the flux of SO_2 molecules into the atmosphere is about 7 orders of magnitude smaller than the sublimation rate of SO_2 in the subsolar region of Io. Thus, surface sputtering by these high-energy ions is insignificant for the overall mass balance of the atmosphere. If minor constituents such as Na and K are present on the surface with the SO_2 frost, then sputtering may be an important mechanism for mobilizing these constituents.

It has been suggested that Na and K exist on the surface of Io in the form of Na_2S and K_2S (ref. 13); however, the surface abundances of these salts are unknown. We consider the consequences of having K, Na, and S present on the surface in cosmic proportions. This assumption implies a number ratio of Na atoms to S atoms of 0.12, and a ratio of K to S of 0.008 (ref. 14). In the sputtering process we assume that each surface constituent is ejected in proportion to its surface abundance. Thus, we estimate the surface source of Na and K to be $\phi_{Na} \simeq 1 \times 10^8$ cm^2 s^{-1} and $\phi_K \simeq 6 \times 10^6$ cm^{-2} s^{-1}. These fluxes are of the correct magnitude to maintain in a steady state the Na and K clouds observed around Io[5-7].

Once in the atmosphere Na and K will escape from Io by the same mechanism that operates for S and O. Earth-based spectroscopic observations of the neutral Na and K clouds indicate particle injection velocities from Io ≥ 3 km s^{-1} (refs 6, 7, 19). Thermal Jean's escape will produce escaping K with

velocities greater than this minimum value only if the exosphere temperature $T_{ex} \geq 14{,}000$ K, while models of Io's ionosphere indicate $T_{ex} \simeq 1{,}000$ K (ref. 1). Sputtering of atmospheric particles by impacting co-rotating S^+ and O^+ will produce an average velocity for the escaping particles ≥ 2.6 km s^{-1}. There are simple and compelling reasons to believe that the exosphere of Io is dominated by neutral oxygen atoms[1] and that Io's exobase lies at more than 2.0 Io radii from the surface[15]. The yield for atmospheric sputtering by low-energy ions is $Y \simeq 1$ (ref. 4). The flux of co-rotating ions averaged over the Io plasma torus is $F_{CR} \simeq 10^{10}$ cm^{-2} s^{-1} (ref. 10). The escaping flux due to atmospheric sputtering is therefore $F_{escape} \geq 9 \times 10^{27}$ O atoms $s^{-1} \simeq 200$ kg s^{-1}. This is sufficient to supply the neutral oxygen cloud that exists along the orbit of Io[16]. Sulphur atoms will be sputtered from the atmosphere in approximately the same proportion in which they exist in the atmosphere at the exobase.

Voyager I measurements of the plasma torus indicate a large but negative radial gradient in the concentration of corotating ions across the orbit of Io[17]. This is of key importance since the flux of sputtered atoms is proportional to the flux of incoming ions. The observed gradient in ion density (and hence co-rotating flux) is sufficiently large that if Io's exobase is located at 2.0 Io radii from its surface, then the flux of sputtered atoms due to impacting S^+ and O^+ is a factor of ~2 greater on Io's inner hemisphere (facing Jupiter) than on the outer hemisphere. Therein may lie a particularly simple explanation of the Na and K ejection asymmetry[18–20]. If Na and K can be supplied to the atmosphere at the required rate, then there should be greatly enhanced atmospheric sputtering of Na, K, O, and S on Io's inner hemisphere. This would lead to ejection asymmetries not only for Na and K (observed) but also for S and O (as yet unobserved).

Many questions remain to be answered in order to understand the details of this two-stage mechanism. For example, how are Na and K species affected by photochemistry and diffusion? What fraction of the atoms sputtered from the surface eventually escape into the torus? What are the characteristics of the asymmetric escape of S and O? These questions provide the basis of a study that is in progress.

We thank J. Trauger, A. Dessler, and A. Summers for helpful discussions; and K. Cherrey for calculations. This research was supported by NASA grants NAGW-202 and NAGW-313. Contribution no. 3873 from the Division of Geological and Planetary Sciences, California Institute of Technology.

Received 11 May; accepted 28 June 1983.

1. Kumar, S. *J. geophys. Res.* **87**, 1677–1684 (1982).
2. Haff, P. K. *et al. J. geophys. Res.* **86**, 6933–6938 (1981).
3. Kumar, S. & Hunten, D. M. in *Satellites of Jupiter* (ed. Morrison, D.) 782–806 (University of Arizona Press, 1982).
4. Haff, P. & Watson, C. C. *J. geophys. Res.* **84**, 8436–8442 (1979).
5. Macy, W. & Trafton, L. *Astrophys. J.* **200**, 510–519 (1975).
6. Brown, R. A. & Yung, Y. L. in *Jupiter* (ed. Gehrels, T.) 1102–1145 (University of Arizona Press, 1976).
7. Trafton, L. *Astrophys. J.* **247**, 1125–1140 (1981).
8. Pearl, J. *et al. Nature* **280**, 755–758 (1979).
9. Kumar, S. *Geophys. Res. Lett.* **7**, 9–12 (1980).
10. Lanzerotti, L. J. *et al. Astrophys. J.* **259**, 920–929 (1982).
11. Melcher, C. L. *et al. Geophys. Res. Lett.* **9**, 1151–1154 (1982).
12. Watson, C. C. & Tombrello, T. A. *Radiat. Effects* (submitted).
13. Fanale, F. P. *et al.* in *Satellites of Jupiter* (ed. Morrison, D.) 756–781 (University of Arizona Press, 1982).
14. Lang, K. R. *Astrophysical Formulae* (Springer, Berlin, 1978).
15. Summers, M. E. & Yung, Y. Preprint (California Institute of Technology, 1983).
16. Shemansky, D. & Smyth, W. *J. geophys. Res.* (submitted).
17. Belcher, J. W. in *Physics of the Jovian Magnetosphere* (ed. Dessler, A.) 68–105 (Cambridge University Press, 1983).
18. Smyth, W. H. & McElroy, M. B. *Astrophys. J.* **226**, 336–346 (1978).
19. Carlson, R. W. *et al. Geophys. Res. Lett.* **10**, 469–472 (1975).
20. Matson, D. L. *Science* **199**, 531–533 (1978).

A new radar auroral backscatter experiment

E. Nielsen*, W. Güttler*, E. C. Thomas†, C. P. Stewart*, T. B. Jones* & A. Hedberg‡

* Max-Planck-Institut für Aeronomie, 3411 Katlenburg-Lindau, FRG
† Department of Astronomy, Leicester University, Leicester, LE1 7RH, UK
‡ Uppsala Ionospheric Observatory, Uppsala, Sweden

In 1982 a new radar auroral backscatter system, SABRE (Sweden and Britain Radar Experiment), commenced operation in northern Europe. Observations with this ground-based system allow estimates to be made of the electric fields in the auroral E-region. As an electric field probe, the coherent radar technique is unique in that measurements are made over a large area (~200,000 km^2) with good spatial resolution (20 × 20 km^2) and with a temporal resolution of typically 20 s. The system field of view covers an *L*-value range 4.3–5.8. This region in the magnetosphere–ionosphere system is now accessible for the first time for detailed electric field studies. We present here observations of two pulsation events.

The auroral radars are sensitive to electrostatic plasma waves in the E-region ionosphere. The mean Doppler shift of the frequency of the transmitted radar signal is closely related to the phase velocity of these waves. The simple fluid theory[1] predicts that the phase velocity in a given direction is equal to the component of the electron drift velocity in that direction. Thus, an analysis of Doppler shifts, observed with radars in a given volume from two independent directions, allows an estimate to be made of the electron drift velocity. Because electrons are $\mathbf{E} \times \mathbf{B}$ drifting at E-region heights, the electric field vector can also be estimated[2].

Recent, more detailed solutions of the basic equations, which govern the plasma waves excited by the two-stream instability[3–5], predict a different, but still deterministic, relationship between the electric field and the observed Doppler shift. Furthermore, new experimental evidence supports qualitatively the predictions of the new theories[6]. As the relationship between the Doppler shifts and the electric field becomes better determined, improved approximations of the latter can be made.

The radar auroral technique used in the SABRE system is similar to the one already used in the STARE (Scandinavian Twin Auroral Radar Experiment) system[7]. This type of system consists of two bi-static radar stations. The Max-Planck Institut für Aeronomie (MPAE), FRG, and Leicester University (LU), UK, have each built one of these radar stations[8]. The German radar is located near Uppsala, Sweden and is operated by MPAE in cooperation with the Uppsala Ionospheric Observatory. The British radar is located near Wick, Scotland, and is operated by LU.

The German radar operates on 142.585 MHz and the British radar on 153.2 MHz. Thus, the radars are sensitive to plasma waves with 1.05 and 0.98 m wavelength, respectively. The lobes from the two transmitter antenna and from the two receiver antenna cover a large common area of the auroral ionosphere (~200,000 km^2). The radar operations are characterized by the parameters listed in Table 1. The accuracy of the directional measurements depends critically on the effectiveness of the isolation between the receiver antenna lobes. The horizontal radiation pattern for the German receiver antenna is reproduced in Fig. 1 and very distinct narrow lobes are evident. In normal operation a sequence consisting of a single-pulse followed by a double-pulse is transmitted with a repetition frequency of 50 mHz. This sequence is continuously executed during the integration time. The averages of the measurements are finally formed and combined[7–9] to yield the backscattered signal intensity (from single pulse pattern) and the mean radial Doppler shift (from double pulse pattern) as a function of lobe

0028–0836/83/340712—03$01.00